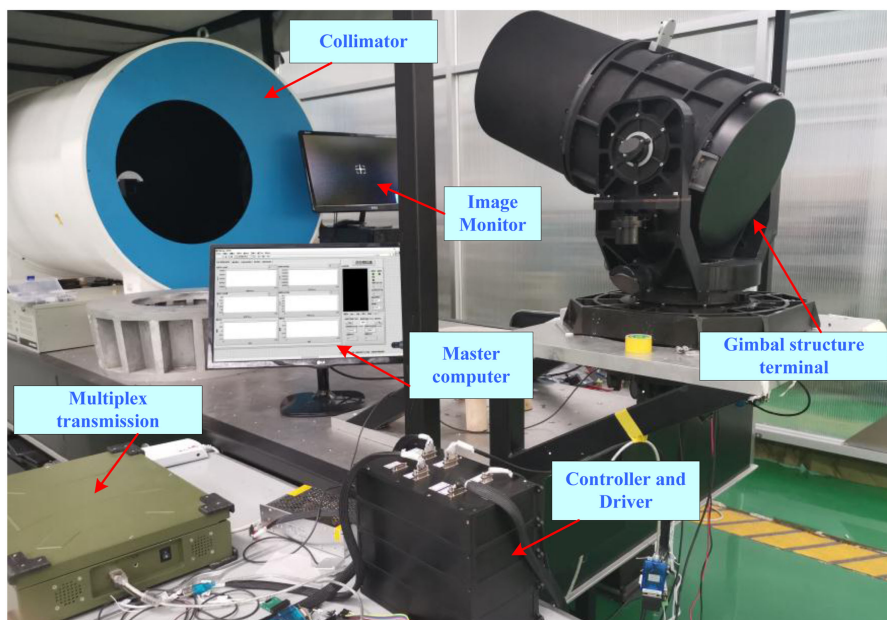🔓**Open Access**

A New Composite Spiral Scanning Approach for Beaconless Spatial Acquisition and Experimental Investigation of Robust Tracking Control for Laser Communication System with Disturbance

Min Zhang
Bo Li
Shoufeng Tong

![IEEE photonics SOCIETY]

![IEEE]

A New Composite Spiral Scanning Approach for Beaconless Spatial Acquisition and Experimental Investigation of Robust Tracking Control for Laser Communication System with Disturbance

Min Zhang [1], **Bo Li,**[2] **and Shoufeng Tong**[3]

[1]School of Opto-Electronic Engineering, Changchun University of Science and Technology, Changchun 130022, China
[2]Institute of Deep-sea Science and Engineering, Chinese Academy of Sciences, Sanya 572000, China
[3]Institute of Space Optoelectronics Technology, Changchun University of Science and Technology, Changchun 130022, China

Abstract: The establishment of laser communication relies on high probability acquisition and then stably track with a high precision. However, the limitation of laser divergence and the interference may lead to unstable acquisition and tracking. In this paper, we proposed a novel beaconless acquisition approach to achieve the coverage of a large uncertainty cone with a narrow communication beam, using a composite spiral scanning method based on fast steering mirror and servomechanism system. The modeling and an analytical expression of sub-regions searching in conjunction with spiral skip overlap are described to realize the effective coverage. A detailed analysis of optimal matching for acquisition parameter is presented to quantify the design result. For the tracking procedure, an experiment is presented to investigate the performance of servo system with the combination of coarse-fine tracking consideration, and iteration learning control scheme in additional to the traditional controller based on periodic external disturbance is introduced for dynamic target tracking system. The iterative control law is taken into account to adjust deviation value and further improve the tracking performance. The obtained tracking accuracy is within $\pm 2\mu$rad which demonstrates the effectiveness the control characteristic in the presence of laser fluctuation.

Index Terms: Optical communication, beaconless spatial acquisition, composite spiral scanning, dynamic tracking assembly, multiple-axis control.

1. Introduction

The beaconless spatial acquisition algorithm and dynamic tracking have received increasing attention mainly due to the system miniaturization design and the platform vibration of communication terminal [1]–[3]. In the process of establishing a laser link, the transmitted laser beam cannot be

pointed precisely at the communication partner because of pointing uncertainties and inadequate know of its exact location. Consequently, for the optical transmission system, before the communication begins, a communication beam has to scan over the whole uncertainty region, the terminal corrects the optical axis according to the position offset of the detected spot [4]–[7]. Such as the typical beacon acquisition process for laser communication system, which involves scanning a high power and high divergence angle light over the uncertainty area until the target spot is detected on the sensor and locked on, and then starting a tracking process for a low power and low divergence communication light [8], [9]. However, as the increased data rate, along with the output laser power requirement, which invites to research the feasibility of beaconless acquisition system, this study is to investigate a new acquisition method where the beacon laser is eliminated entirely, and instead of using the narrow communication beam for acquisition [10]–[13]. We concentrate on beaconless acquisition with a spiral scanning method combining two actuators for improving the coverage of a large uncertainty cone with a narrow communication beam, and the appropriate mathematical models and the corresponding analysis are presented to describe this scan pattern.

To deal with the system disturbances, an iterative learning control is applied in conjunction with the traditional PI controller, this control algorithm is presented to implement dynamic target tracking and performance improvement [14]–[17]. The purpose is to generate a compensation reference to achieve superior tracking for fluctuation laser target, meanwhile, this control method is capable of reduction for the periodic disturbance. The proposed scheme is implemented and the corresponding performance can be evaluated through experimental investigations. The experimental response for periodic external disturbance demonstrate the ability of error rejection, and also validate the effectiveness of the proposed target tracking controller.

The main objective of this paper is to describe the proposed composite acquisition and tracking approach based on spiral patterns and the actuators. The discussion is given with beaconless acquisition analysis of narrow beam-width and the dynamic tracking algorithm, including the scanning method modeling and characteristic analysis, and also contains the suppression ability of iterative learning control strategy in moving platform tracking, as well as the improvement of track precision of laser communication link.

2. Experimental Setup Description

In order to examine the feasibility of this novel concept of composite spiral beaconless acquisition and the effect of fluctuation target tracking. A photograph of the experimental setup is given in Fig. 1, in which a uni-directional near horizontal laser link is established between the transmitting collimator device and the receiving terminal. This configuration is a conventional design to implement the validation of the proposed acquisition method and dynamic track algorithms.

As shown in Fig. 1, a laser beam propagates through collimator to produce parallel rays and simulate infinite distance, and a two-dimensional reflector is located at this optical path which is used to induce the effect of laser fluctuation characteristic. The receiver contains a CMOS detection sensor that generates the line-of-sight (LOS) error of the incoming light for performing beaconless acquisition and tracking functions. The external aperture of the communication terminal is 300mm, and this gimbal structure has a large operating range, the azimuth angular range is $\pm 180°$, and the elevation angular range is $150°$. All the optical elements and receive units are mounted to the inner gimbal structure. The low frequency angular motions are mainly accomplished by the coarse pointing assembly (CPA). Fine pointing assembly (FPA) is a single-mirror, wide bandwidth, and two-axis fast steering mirror device with a deflection angle of 2 mrad (related to the acquisition sub-region), which is capable of operating at a high servo bandwidth and can complete high frequency angular movement. As the core executive actuator, FPA can be used to cope with the external interference during dynamic tracking.

Owing to the design of the signal light's angle of divergence and the limitation of terminal acquisition's field of view (FOV), so that during the establishment of the communication link, the communication laser cannot be acquired directly without scanning the uncertainty cone. In fact, a single CMOS sensor is employed for performing composite coarse-fine tracking, and we also
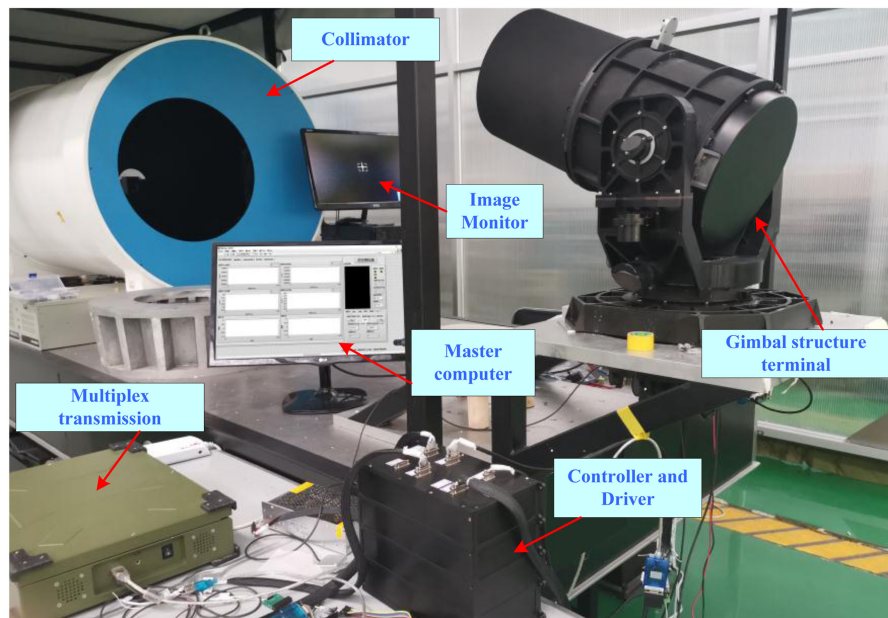
Fig. 1. Experimental platform photograph of the communication terminal prototype.

design the system structure which eliminates the beacon light, such a combination enables a unique communication system of miniaturization and lightweight. Therefore, during the acquisition phase, the high speed FPA actuator can also be used to scan the sub-regions rapidly which is equivalent to achieve the increasing of laser divergence angle. Moreover, due to the fact that the acquisition uncertainty area is so large that this sub-region scanned by FPA also cannot completely cover it. So it is necessary to combine the CPA mechanism that with a wider executive range. Compared with the beacon acquisition, this combination approach also reduces the need for the coarse pointing assembly, with this method, the total scan time can be further decreased. Thus, it is important to analyze the impact of such a small divergence beam in the beaconless acquisition process, and in order to establish a stable laser link, it is also necessary to provide an appropriate dynamic tracking compensation algorithm, and using the experimental results to verify the ability of disturbance rejection.

3. Beaconless Spatial Acquisition Algorithm and Scanning Characteristic Analysis

3.1. Laser Spiral Acquisition Modeling and Composite Scanning for Terminal Actuators

The beaconless spatial acquisition algorithm studied in this paper allows the design of a laser communication terminal without a dedicated beacon beam. During the procedure of acquisition, different scanning patterns have different characteristics, especially when using small divergence angle light to achieve beaconless acquisition, the selection of search pattern might be directly affect both duration and reliability.

This paper presents a scanning method combining two actuators of CPA and FPA, sub-regions scanning and stepping overlap. Thus, spiral scan pattern is chosen as it scans from the high probability location to the least likely location. In order to define the scan trajectory during the procedure of acquisition, we must present an appropriate mathematical model to describe the spiral scan.

Target acquisition is related to the beam divergence and the size of uncertainty cone, and acquisition probability depends on the effective coverage [19]. Consider now the radial and angular

velocity expressions of spiral scan can be modeled approximately by the equations as

$$v_r = \sqrt{\frac{(1-k)\,\theta_{uc}\theta_{div}^2}{2\pi t\,(\theta_{uc}-\theta_{div})\,T_{dwell}}} \tag{1}$$

$$v_\theta = \sqrt{\frac{2\pi\,(\theta_{uc}-\theta_{div})}{(1-k)\,\theta_{uc}t T_{dwell}}} \tag{2}$$

where k is the beam overlap factor, T_{dwell} is the laser dwell time, that is related to the received power and exposure time of tracking camera, θ_{uc} and θ_{div} are the uncertainty cone and laser divergence beamwidth, respectively.

The functions of v_r in (1) and v_θ in (2) can be combined to expressed to the two dimension coordinate points of scanning pattern with time-varying, as described in (3) and (4), which forms the basis of the proposed double-actuator spiral acquisition strategy

$$x = v_r t \cos(v_\theta t) \tag{3}$$

$$y = v_r t \sin(v_\theta t) \tag{4}$$

The horizontal and vertical dwell points that expressed above are independent with each other. And this kind of linear velocity scan can develop an expression for the number of rings as a function of uncertainty cone and laser divergence, as given in the following equation

$$N_{scan} = \frac{\theta_{uc}-\theta_{div}}{2\,(1-k)\,\theta_{div}} \tag{5}$$

The scan time from initial point to the searching end can be calculated by the following equation

$$T_{spiral} = \frac{\pi\,T_{dwell}}{2\,(1-k)}\left[\left(\frac{\theta_{uc}}{\theta_{div}}\right)^2 - \frac{\theta_{uc}}{\theta_{div}}\right] \tag{6}$$

3.2. Analysis and Optimization Matching for Spiral Scanning Parameters of CPA and FPA

To explain this optimal matching approach, we divide beaconless acquisition process into two procedures: the signal light searching in sub-regions, and CPA actuator spiral skip scanning. The block diagram for beaconless spatial acquisition with the combination spiral of CPA and FPA is illustrated in Fig. 2. We can see each component of function is designed according to the above formulas. Here, the labview software is used to complete the simulation work of beaconless acquisition process based on the proposed scanning algorithm. Compared with the spiral and raster scanning pattern in reference [18], a more innovation composite spiral method is adopted here, the unnecessary scanning area is removed from this proposed method, as shown in Fig. 2, each spiral spot of CPA represents a location of sub-region, considering the suitable overlap between the sub-region areas in order to ensure the effective coverage. Under normal conditions with sufficient optical power (without considering coupled with vibration, the details about beaconless acquisition with vibration can be found in reference [18]), the signal light spot will be recognized during the scanning coverage process of uncertainty cone. Consequently, it can be seen that spiral scan is more efficient than others. The corresponding spiral scanning patterns are illustrated in Fig. 3 and Fig. 4 below, respectively, in which the lines appear to be simple which decrease the complexity of the terminal for searching.

Table 1 present the parameters matching results with the combination spiral scanning, from which it can be seen that the proposed beam searching approach can meet the desired perfor-mance criteria of scan coverage. Sub-region scan pattern (see Fig. 3) based on the FPA actuator (S-330 piezo tip/tilt platform) is for a diameter of 1.2 mrad, a beam divergence of 0.1 mrad, and a 40% overlap to prevent small divergence angle from causing leakage which can guarantee the acquisition probability. The spot dwell time of each sample location is set to 1.8ms, taking into account the integration time (500 μs) of the CMOS imaging camera (MV1-D1024E CameraLink).
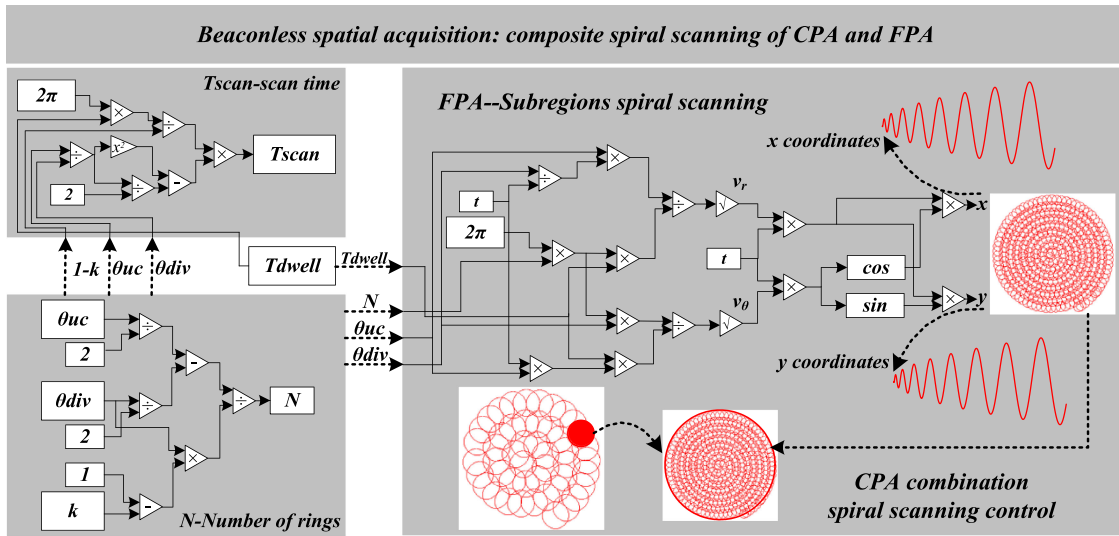
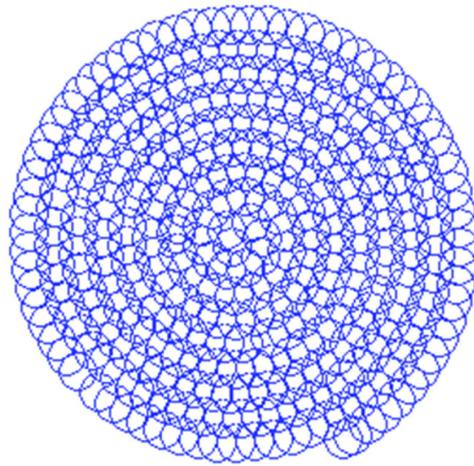Fig. 2. The diagram of beaconless acquisition based on the composite spiral of CPA and FPA.

Fig. 3. FPA sub-regions spiral scanning.

TABLE 1
Parameters of Beaconless Acquisition With the Composite Spiral Scanning

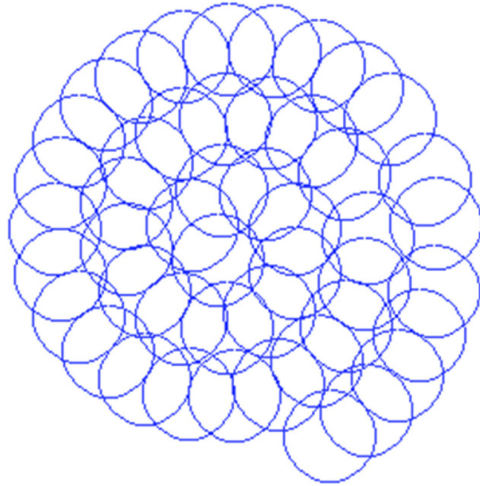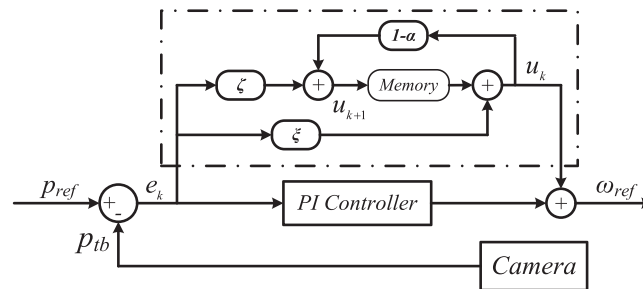| Acquisition parameter	FPA	CPA
Uncertainty cone	1.2mrad	4.3mrad
Laser divergence beamwidth	0.1mrad	1.2mrad
Tip/tilt angle	2mrad	2.6rad
Beam overlap factor	40%	35%
Laser dwell time	1.8ms	650ms
Number of rings	9	3
Servo bandwidth	1200Hz	13Hz
Sub-region scanning time	0.62s	27.8s

Fig. 4 . CPA combination spiral scanning.

Fig. 5. Control structure block diagram of dynamic target tracking.

The scan time of a sub-region is then 0.62 second. This high acceleration actuator also can provide a high-bandwidth (hundreds of hertz) and assure the precision of optimal angular motion. CPA combination spiral scanning (see Fig. 4) is for a diameter of 4.3 mrad, a beam divergence of 1.2 mrad, and a 35% overlap factor. Here, the only way to obtain overlap areas between two spirals is by numerical evaluation or by simulation. The CPA dwell time of each sample location is set to 650ms, taking into account the sub-regions scan time (620ms) of the FPA. The main beaconless acquisition parameters are summarized in Table 1. Correlation statistics are derived to help quantify the result. In addition, the terminal corrects the optical axis according to the position offset of the detected spot. After several corrections, this beaconless procedure enables the terminal to lock on to the signal light, and ending successfully with tracking state. This will be discussed next.

4. Target Laser Tracking Performance in the Presence of External Interference

4.1 Track the Signal Light by the Iterative Learning Control Method

The application of iterative learning control is a relatively new strategy to improve the tracking performance for modeling uncertainty system, especially in response to periodic external interference of communication servomechanism system. Such an external disturbance rejection and target tracking controller takes the form as shown in Fig. 5, a memory is used to store the control input for the next operating cycle, in which the reduction of tracking error between the desired output and the real-time feedback can be guaranteed iteration by iteration.

A block diagram description as shown in Fig. 5, to achieve superior tracking for fluctuation laser target, an iterative learning control is required in addition to the traditional PI controller. The outmost track loops are used per axis to compensate and correct the azimuth and elevation LOS axes by obtaining the feedback error signals from the camera sensor. The angular displacement which passes through the iterative learning controller will generate the reference command for the inner rate loop, and then after speed closed loop control a motor driving torque is produced in order to null the position error and achieve a stable track.

In this study, the objective is to design a controller for disturbance to improve tracking performance. For a qualitative description of iteration learning control, the dynamic system is described parametrically as the following state-space equation

$$\begin{cases} \dot{x}(t) = ax(t) + bu(t) + \eta(t) \\ y(t) = cx(t) \end{cases} \tag{7}$$

where $x(t)$ and $y(t)$ correspond to the system state variable and the system output, $u(t)$ and $\eta(t)$ represent the control input and the external uncertainties due to periodic perturbations.

For the iterative learning control, when G is given as the learning gain, the convergence condition should be satisfied to ensure the control law, and the communication system will asymptotically stable if

$$\|I - cbG\| < 1 \tag{8}$$

According to the configuration for iterative learning tracking approach, using this principle, the control law can be designed to adjust deviation value and achieve compensation, which can be updated as the following equation

$$u_{k+1}(t) = (1 - \alpha)u_k(t) + \zeta e_k(t) + \xi e_{k+1}(t) \tag{9}$$

where ζ and ξ represent the gain coefficients for position deviation at k_{th} and $(k+1)_{th}$ iteration, respectively, and α is a forgetting factor to increase the robustness of the algorithm against interference.

The terminal rotation equation can be obtained as

$$J\frac{d\omega}{dt} + T_L + B_m\omega = T_e \tag{10}$$

where ω is the rotation speed, J and B_m are the inertia and friction coefficient, T_L and T_e are load torque and motor torque, and $T_e = k_t i_q$, k_t is the torque constant.

Using equation (10) yields the motor of dynamics, and can be expressed as

$$\dot{\omega} = -\frac{B_m}{J}\omega + \frac{k_t}{J}i_q - \frac{1}{J}T_L \tag{11}$$

Substituting (11) into (7), and together with (8), the convergence condition for this dynamic target tracking system can be written as

$$\left\| 1 - \frac{k_t}{J}\zeta \right\| < 1 \tag{12}$$

Although a detailed mathematical model is not required, knowing of the plant is particularly helpful for the stability characteristic analysis. Here, in this system $k_t = 0.7$Nm/A, $J = 0.03$kgm^2, according to the criterion condition in (12), the parameter ζ of the correction algorithm should be designed reasonably, which can ensure the stability of the system.

4.2 Multiple-axis Tracking Performance and Dynamic Target Tracking Results

The experiment has been carried out using the proposed iteration learning control scheme based on the servomechanism system that described in previous section 2. The main objective is to describe the interference suppression ability of the dynamic tracking algorithm and the improvement of tracking precision for the laser beam. In this section, several experimental results have
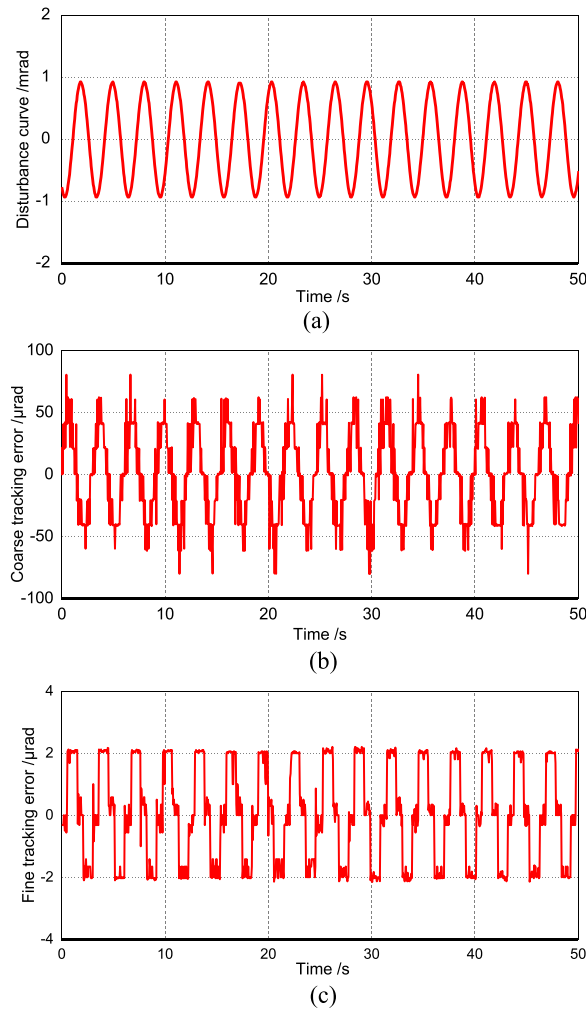
Fig. 6. Dynamic coarse and fine tracking performance with external disturbance (vibration amplitude: $-0.87\sim+0.87$ mrad, maximum acceleration: 3.82 mrad/s^2).

been obtained under different interference amplitudes and frequencies, as shown in Fig. 6-9, these graphs are presented to verify the effectiveness of iteration learning control strategy. In order to suppress external interference effectively, the classical PI control method is used in the internal rate and current loop due to stability considerations, the sampling times for speed and current controllers are 800µs and 66µs, respectively. And the corresponding gains are designed as: speed controller: $k_{vp} = 1.7$, $k_{vi} = 0.3$, current controller: $k_{cp} = 2.8$, $k_{ci} = 0.6$, the control parameters for the tracking loop are: the gains of PI are: $k_p = 1.6$, $k_i = 0.3$, the learning gains are: $\zeta = 0.05$, $\xi = 0.03$, the forgetting factor $\alpha = 0.12$.

The configuration of this experimental system consists of a dynamic tracking mode using the combination of coarse and fine tracking, in which the tracking camera feedback the image miss-distance according to the received light spot, then the control value is computed based on the controller gains and output to the driving system. The incident laser with disturbance is the independent contribution to vibration bias for each axis. When the laser fluctuation condition and experimental setting are determined, during the operation, the tracking interference and residual error variables are recorded including the monitoring of laser disturbance waveform, coarse following error, and the fine tracking error.
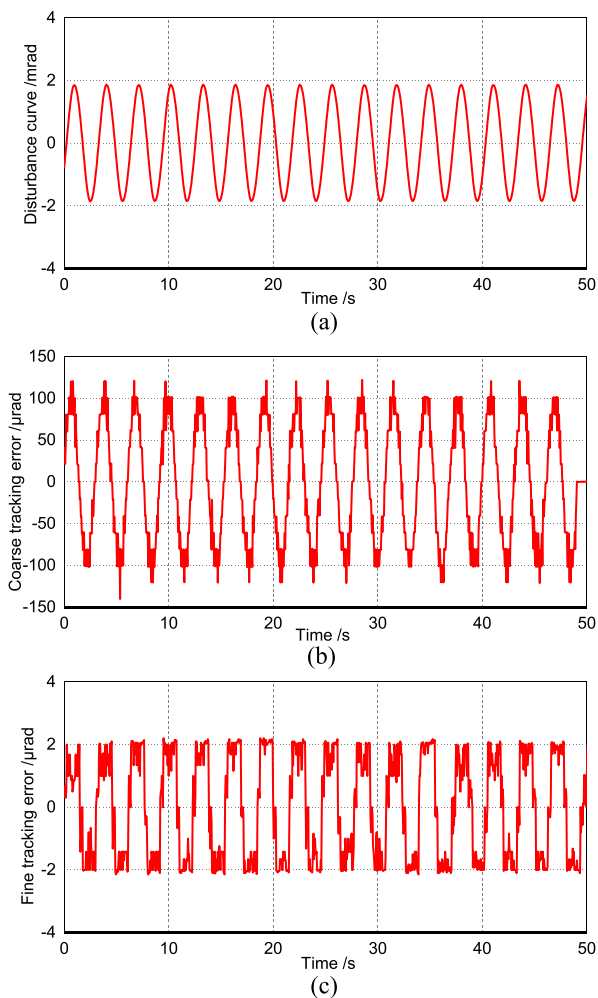
Fig. 7. Dynamic coarse and fine tracking performance with external disturbance (vibration amplitude: $-1.74\sim+1.74$ mrad, maximum acceleration: 7.64 mrad/s^2).

Partial experimental data has been illustrated as shown in the following Fig. 6, 7, 8, and 9, each graph consists of three subplots, the relevant data is shown in it, including the laser fluctuation curve that propagates through collimator (in the top row of each graph), coarse following error curve for the gimbal structure terminal (in the middle row of each graph), and the combination of coarse-fine tracking precision waveform (on the bottom row of each graph). In order to explain the tracking performance in presence of disturbance, it is necessary to analyze and examine the interference suppression controller by using disturbance tracking conditions with different amplitudes and frequencies, and the tracking errors can be applied to evaluate the robustness for communication servo system. Fig. 6 and 7 present the experimental research results which were performed at the disturbance with the maximum acceleration of 3.82 mrad/s^2 and 7.64 mrad/s^2, respectively, Fig. 6(a) and 7(a) show the position oscillation trajectory of laser source caused by a two dimensional tip/tilt platform in the collimator, Fig. 6(a) shows an external laser vibration ranging from $-0.87\sim+0.87$ mrad, and Fig. 7(a) shows the vibration waveform in which the vibration is set from $-1.74\sim+1.74$ mrad. As shown in Fig. 6(b) and 7(b), it appears that the coarse following error changes from -80 μrad~80 μrad (see Fig. 6(b)) and -120 μrad~120 μrad (see Fig. 7(b)). Both Fig. 6(c) and 7(c) show that the composite tracking is utilized to suppress the external disturbance and can improve the tracking accuracy within ±2μrad.
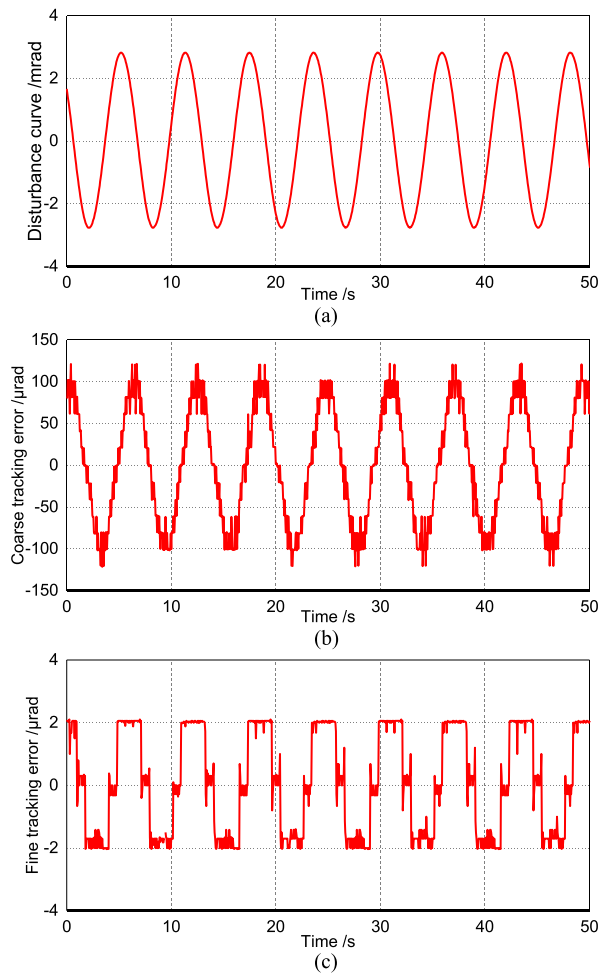
Fig. 8. Dynamic coarse and fine tracking performance with external disturbance (vibration amplitude: $-2.61\sim+2.61$ mrad, maximum acceleration: 2.86 mrad/s^2).

The aforementioned tracking results demonstrate the disturbance rejection and the uncertainties compensation ability of iteration learning control. Furthermore, Fig. 8 and 9 which is conducted for verifying the robustness characteristic are arranged in the same sequence, they are presented to illustrate that the proposed method can ensure smooth and high accuracy experimental results based on different operation conditions, which are also derived from the dynamic target tracking method mentioned above. Fig. 8(a) and 9(a) summarize the tracking data based on another two kinds of different oscillation waves, with the maximum acceleration of 2.86 mrad/s^2 and 0.81 mrad/s^2, respectively. Fig. 8(a) shows an external laser vibration ranging from -2.61$\sim$+2.61 mrad, and Fig. 9(a) shows the vibration waveform in which the vibration is set from -5.22$\sim$+5.22 mrad. As shown in Fig. 8(b) and 9(b), it appears that the coarse following error changes from -125 μrad$\sim$125 μrad (see Fig. 8(b)) and -100 μrad$\sim$100 μrad (see Fig. 9(b)). Subsequently, comparing the test results in Fig. 8(c) and 9(c), when steady-state track is reached, it can be observed that the fine tracking errors also can be suppressed to 2 μrad in these higher vibration ranges. Moreover, significant improvement of tracking performance is achieved. Therefore, system tracking error analysis was performed on the tracking residuals of the fine tracking subsystem. Then track on the incident beam, thereby forming a communication link.
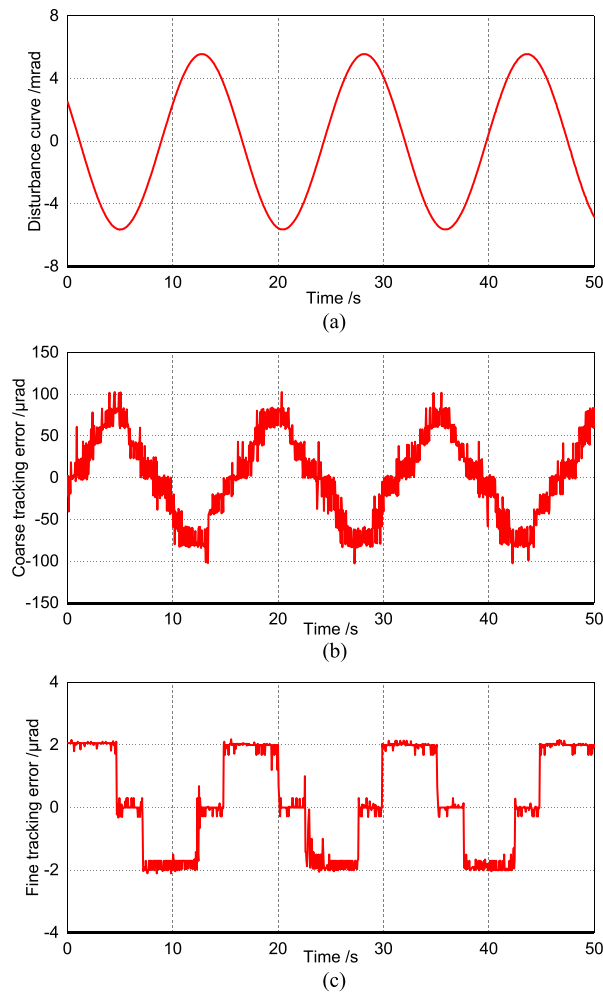
Fig. 9. Dynamic coarse and fine tracking performance with external disturbance (vibration amplitude: $-5.22 \sim +5.22$ mrad, maximum acceleration: 0.81 mrad/s^2).

5. Conclusion

A uni-directional near horizontal laser link was conducted to investigate the proposed beaconless composite spiral scanning and dynamic tracking algorithms. The beaconless acquisition process is introduced based on the communication light spiral searching in sub-regions with FPA and referring to the CPA actuator implement spiral skip scanning in the whole uncertainty cone. The parameters matching results and its application analysis have been summarized for this novel combination of spiral scanning approach. A periodic disturbance rejection scheme using iteration learning control which is presented in this paper to achieve superior tracking for fluctuation laser target of communication servomechanism system. The proposed control structure has been applied to the composite track process for improving the tracking accuracy. The experimental results have been illustrated which consist of four cases collected including laser fluctuation trajectory with different amplitudes and peak acceleration settings. Comparing the test results, significant tracking and disturbance suppression performance are achieved, and also can improve the tracking accuracy within ± 2 μrad, which can verify the robustness characteristic of the system. Additional complicated optic axis correction approach and different disturbance range can be derived in the future works. The analysis results of beaconless acquisition have been presented to demonstrate the effectiveness of the composite spiral of CPA and FPA, and the experimental results have been

given with high tracking accuracy in order to verify the effectiveness of iteration learning control in suppressing laser disturbance.

Acknowledgment

References

[1] D. Dallmann, M. Reinhardt, M. Gregory, F. Heine, U. Sterr, and R. Meyer, "GEO-LEO beaconless spatial acquisition reality in space," in *Proc. IEEE Int. Conf. Space Opt. Syst. Appl.*, 2015.

[2] Q. Li, L. Liu, X. Ma, S. Liu, H. Yun, and S. Tang, "Development of multitarget acquisition, pointing, and tracking system for airborne laser communication," *IEEE Trans. Ind. Informat.*, vol. 15, no. 3, pp. 1720–1729, Mar. 2019.

[3] Q. Wang, S. Yu, L. Tan, and J. Ma, "Approach for recognizing and tracking beacon in inter-satellite optical communication based on optical flow method," *Opt. Express*, vol. 26, no. 21, pp. 28080–28090, 2018.

[4] K. Xu and Y. Ou, "Theoretical and numerical characterization of a 40 gbps long-haul multi-channel transmission system with dispersion compensation," *Digit. Commun. Netw.*, vol. 1, no. 3, pp. 222–228, 2015.

[5] Q. Wang, J. Ma, L. Tan, and S. Yu, "Quick topological method for acquiring the beacon in inter-satellite laser communications," *Appl. Opt.*, vol. 53, no. 33, pp. 7863–7867, 2014.

[6] M. Li, C. Zeng, J. Lei, Y. Guo, and M. Li, "Effect of external mismatch and internal mismatch caused by pointing error on performances of space chaos laser communication system," *Opt. Express*, vol. 28, no. 5, pp. 6146–6163, 2020.

[7] T. Song, Q. Wang, M. W. Wu, T. Ohtsuki, M. Gurusamy, and P. Kam, "Impact of pointing errors on the error performance of inter-satellite laser communications," *J. Lightw. Technol.*, vol. 35, no. 14, pp. 3082–3091, 2017.

[8] S. Yu, F. Wu, Q. Wang, L. Tan, and J. Ma, "Theoretical analysis and experimental study of constraint boundary conditions for acquiring the beacon in satellite-ground laser communications," *Opt. Commun.*, vol. 40, no. 2, pp. 585–592, 2017.

[9] Q. Wang, Y. Liu, J. Ma, L. Tan, S. Yu, and C. Li, "Quick acquisition and recognition method for the beacon in deep space optical communications," *Appl. Opt.*, vol. 55, no. 34, pp. 9738–9743, 2016.

[10] X. Li, S. Yu, J. Ma, and L. Tan, "Analytical expression and optimization of spatial acquisition for intersatellite optical communications," *Opt. Express*, vol. 19, no. 3, pp. 2381–2390, 2011.

[11] U. Sterr, M. Gregory, and F. Heine, "Beaconless acquisition for ISL and SGL, summary of 3 years operation in space and on ground," in *Proc. IEEE Int. Conf. Space Opt. Syst. Appl.*, pp. 38–43, 2011.

[12] S. Bai, J. Qiang, L. Zhang, and J. Wang, "Optimization of spatial acquisition systems for low-light-level robustness in space optical communications," *Opt. Lett.*, vol. 40, no. 16, pp. 3750–3753, 2015.

[13] H. Su *et al.*, "RoF transport systems with OSNR enhanced multi-band optical carrier generator," *Opt. Express*, vol. 19, no. 19, pp. 18516–18522, 2011.

[14] Y. X. Su, C. H. Zheng, and B. Y. Duan, "Automatic disturbances rejection controller for precise motion control of permanent-magnet synchronous motors," *IEEE Trans. Ind. Electron.*, vol. 52, no. 3, pp. 814–823, Jun. 2005.

[15] D. Wu and K. Chen, "Design and analysis of precision active disturbance rejection control for noncircular turning process," *IEEE Trans. Ind. Electron.*, vol. 56, no. 7, pp. 2746–2753, Jul. 2009.

[16] V. A. Skormin, M. A. Tascillo, and D. J. Nicholson, "Jitter rejection technique in a satellite-based laser communication system," *Opt. Eng.*, vol. 32, no. 11, pp. 2764–2769, 1993.

[17] G. Baister, P. Gatenby, J. Lewis, and M. Witting, "The SOUT optical intersatellite communication terminal," *IEE Proc. Optoelectron*, vol. 141, no. 6, pp. 345–355, Dec. 1994.

[18] Y. Teng, M. Zhang, and S. Tong, "The optimization design of sub-regions scanning and vibration analysis for beaconless spatial acquisition in the inter-satellite laser communication system," *IEEE Photon. J.*, vol. 10, no. 6, Dec. 2018, Art. no. 7909611.

[19] K. Xu, "Monolithically integrated si gate-controlled light-emitting device: Science and properties," *J. Opt.*, vol. 20, no. 2, pp. 1–8, 2018.